

Production of heavy and superheavy nuclei in massive fusion reactions

Zhao-Qing Feng^{1*}, Gen-Ming Jin¹, Jun-Qing Li¹, Werner Scheid²

¹*Institute of Modern Physics, Chinese Academy of Sciences, Lanzhou 730000, China*

²*Institut für Theoretische Physik der Universität, 35392 Giessen, Germany*

Abstract

Within the framework of a dinuclear system (DNS) model, the evaporation-residue excitation functions and the quasi-fission mass yields in the ^{48}Ca induced fusion reactions are investigated systematically and compared with available experimental data. Maximal production cross sections of superheavy nuclei based on stable actinide targets are obtained. Isotopic trends in the production of the superheavy elements $Z=110, 112-118$ based on the actinide isotopic targets are analyzed systematically. Optimal evaporation channels and combinations as well as the corresponding excitation energies are proposed. The possible factors that influencing the isotopic dependence of the production cross sections are analyzed. The formation of the superheavy nuclei based on the isotopes U with different projectiles are also investigated and calculated.

PACS: 25.70.Jj, 24.10.-i, 25.60.Pj

Keywords: DNS model; evaporation-residue excitation functions; ^{48}Ca induced fusion reactions; isotopic trends

1 Introduction

The synthesis of heavy or superheavy nuclei is a very important subject in nuclear physics motivated with respect to the island of stability which is predicted theoretically, and has obtained much experimental research with the fusion-evaporation reactions [1, 2]. The existence of the

*Corresponding author.

E-mail address: fengzhq@impcas.ac.cn

superheavy nucleus (SHN) ($Z \geq 106$) is due to strong binding shell effects against the large Coulomb repulsion. However, the shell effects get reduced with increasing the excitation energy of the formed compound nucleus. Combinations with a doubly magic nucleus or nearly magic nucleus are usually chosen owing to the larger reaction Q values. Reactions with ^{208}Pb or ^{209}Bi targets were first proposed by Oganessian et al. to synthesize SHN [3]. Six new elements with $Z=107-112$ were synthesized in cold fusion reactions for the first time and investigated at GSI (Darmstadt, Germany) with the heavy-ion accelerator UNILAC and the SHIP separator [1, 4]. Recently, experiments on the synthesis of element 113 in the $^{70}\text{Zn}+^{209}\text{Bi}$ reaction have been performed successfully at RIKEN (Tokyo, Japan) [5]. However, it is difficult to produce heavier SHN in the cold fusion reactions because of the smaller production cross sections that are lower than 1 pb for $Z > 113$. Other possible ways to produce SHN are very needed to be investigated in experimentally and theoretically. Recently, the superheavy elements $Z=113-116, 118$ were synthesized at FLNR in Dubna (Russia) with the double magic nucleus ^{48}Ca bombarding actinide nuclei [6, 7, 8]. New heavy isotopes ^{259}Db and ^{265}Bh have also been synthesized at HIRFL in Lanzhou (China) [9]. Further experimental works are necessary in order to testify the new synthesized SHN. A reasonable understanding of the formation of SHN in the massive fusion reactions is still a challenge for theory.

In accordance with the evolution of two heavy colliding nuclei, the dynamical process of the compound nucleus formation and decay is usually divided into three reaction stages, namely the capture process of the colliding system to overcome the Coulomb barrier, the formation of the compound nucleus to pass over the inner fusion barrier, and the de-excitation of the excited compound nucleus by neutron emission against fission. The transmission in the capture process depends on the incident energy and relative angular momentum of the colliding nuclei, which is the same as that in the fusion of light and medium mass systems. The complete fusion of the heavy system after capture in competition with quasi-fission is very important in the estimation of the SHN production. The concept of the "extra-push" energy explains for the fusion of two heavy colliding nuclei in the macroscopic dynamical model [10, 11]. At present it is still difficult to make an accurate description of the fusion dynamics. After the capture and the subsequent evolution to form the compound nucleus, the thermal compound nucleus will decay by the emission of light particles and γ rays against fission. The three stages will affect the formation of evaporation residues observed in laboratories. The evolution of the whole process of massive heavy-ion collisions is very complicated at near-barrier energies. Most of the theoretical methods on the formation of SHN have a similar viewpoint in the description of the capture and the de-excitation

stages, but there are different description of the compound nucleus formation process. There are mainly two sorts of models, depending on whether the compound nucleus is formed along the radial variable (internuclear distance) or by nucleon transfer in a touching configuration which is usually the minimum position of the interaction potential after capture of the colliding system. Several transport models have been established to understand the fusion mechanism of two heavy colliding nuclei leading to SHN formation, such as the macroscopic dynamical model [10, 11], the fluctuation-dissipation model [12], the concept of nucleon collectivization [13] and the dinuclear system model [14, 15]. Recently, the improved isospin-dependent quantum molecular dynamics (ImIQMD) model was also proposed to investigate the fusion dynamics of SHN [16, 17]. With these models experimental data can be reproduced to a certain extent, and some new results have been predicted. However, these models differ from each other, and sometimes different physical ideas are used.

Further improvements of these models have to be made. Here we use a dinuclear system (DNS) model [15, 18], in which the nucleon transfer is coupled with the relative motion by solving a set of microscopically derived master equations, and a barrier distribution of the colliding system is introduced in the model. We present a new and extended investigation of the production of superheavy nuclei in the ^{48}Ca induced fusion reactions and in other combinations.

In Section 2 we give a simple description on the DNS model. Calculated results of fusion dynamics and SHN production are given in Section 3. In Section 4 conclusions are discussed.

2 Dinuclear system model

The dinuclear system [19] is a molecular configuration of two touching nuclei which keep their own individuality [14]. Such a system has an evolution along two main degrees of freedom: (i) the relative motion of the nuclei in the interaction potential to form the DNS and the decay of the DNS (quasi-fission process) along the R degree of freedom (internuclear motion), (ii) the transfer of nucleons in the mass asymmetry coordinate $\eta = (A_1 - A_2)/(A_1 + A_2)$ between two nuclei, which is a diffusion process of the excited systems leading to the compound nucleus formation. Off-diagonal diffusion in the surface (A_1, R) is not considered since we assume the DNS is formed at the minimum position of the interaction potential of two colliding nuclei. In this concept, the evaporation residue cross section is expressed as a sum over partial waves with angular momentum

J at the centre-of-mass energy $E_{c.m.}$,

$$\sigma_{ER}(E_{c.m.}) = \frac{\pi \hbar^2}{2\mu E_{c.m.}} \sum_{J=0}^{J_{max}} (2J+1) T(E_{c.m.}, J) P_{CN}(E_{c.m.}, J) W_{sur}(E_{c.m.}, J). \quad (1)$$

Here, $T(E_{c.m.}, J)$ is the transmission probability of the two colliding nuclei overcoming the Coulomb potential barrier in the entrance channel to form the DNS. In the same manner as in the nucleon collectivization model [13], the transmission probability T is calculated by using the empirical coupled channel model, which can reproduce very well available experimental capture cross sections [13, 15]. The P_{CN} is the probability that the system will evolve from a touching configuration into the compound nucleus in competition with quasi-fission of the DNS and fission of the heavy fragment. The last term is the survival probability of the formed compound nucleus, which can be estimated with the statistical evaporation model by considering the competition between neutron evaporation and fission [15]. We take the maximal angular momentum as $J_{max} = 30$ since the fission barrier of the heavy nucleus disappears at high spin [20].

In order to describe the fusion dynamics as a diffusion process in mass asymmetry, the analytical solution of the Fokker-Planck equation [14] and the numerical solution of the master equations [21, 22] have been used, which were also used to treat deep inelastic heavy-ion collisions [23]. Here, the fusion probability is obtained by solving a set of master equations numerically in the potential energy surface of the DNS. The time evolution of the distribution function $P(A_1, E_1, t)$ for fragment 1 with mass number A_1 and excitation energy E_1 is described by the following master equations [18, 21],

$$\frac{dP(A_1, E_1, t)}{dt} = \sum_{A'_1} W_{A_1, A'_1}(t) \left[d_{A_1} P(A'_1, E'_1, t) - d_{A'_1} P(A_1, E_1, t) \right] - \left[\Lambda^{gf}(\Theta(t)) + \Lambda^{fis}(\Theta(t)) \right] P(A_1, E_1, t). \quad (2)$$

Here W_{A_1, A'_1} is the mean transition probability from the channel (A_1, E_1) to (A'_1, E'_1) , and d_{A_1} denotes the microscopic dimension corresponding to the macroscopic state (A_1, E_1) . The sum is taken over all possible mass numbers that fragment A'_1 may take (from 0 to $A = A_1 + A_2$), but only one nucleon transfer is considered in the model with $A'_1 = A_1 \pm 1$. The excitation energy E_1 is the local excitation energy ε_1^* with respect to fragment A_1 , which is determined by the dissipation energy from the relative motion and the potential energy of the corresponding DNS and will be shown later in Eqs.(8) and (9). The dissipation energy is described by the parametrization method of the classical deflection function [24, 25]. The motion of nucleons in the interacting potential is governed by the single-particle Hamiltonian [15, 21]:

$$H(t) = H_0(t) + V(t) \quad (3)$$

with

$$\begin{aligned}
H_0(t) &= \sum_K \sum_{\nu_K} \varepsilon_{\nu_K}(t) a_{\nu_K}^\dagger(t) a_{\nu_K}(t), \\
V(t) &= \sum_{K,K'} \sum_{\alpha_K, \beta_{K'}} u_{\alpha_K, \beta_{K'}}(t) a_{\alpha_K}^\dagger(t) a_{\beta_{K'}}(t) = \sum_{K,K'} V_{K,K'}(t).
\end{aligned} \tag{4}$$

Here the indices K, K' ($K, K' = 1, 2$) denote the fragments 1 and 2. The quantities ε_{ν_K} and $u_{\alpha_K, \beta_{K'}}$ represent the single particle energies and the interaction matrix elements, respectively. The single particle states are defined with respect to the centers of the interacting nuclei and are assumed to be orthogonalized in the overlap region. So the annihilation and creation operators are dependent on time. The single particle matrix elements are parameterized by

$$u_{\alpha_K, \beta_{K'}}(t) = U_{K,K'}(t) \left\{ \exp \left[-\frac{1}{2} \left(\frac{\varepsilon_{\alpha_K}(t) - \varepsilon_{\beta_{K'}}(t)}{\Delta_{K,K'}(t)} \right)^2 \right] - \delta_{\alpha_K, \beta_{K'}} \right\}, \tag{5}$$

which contain some parameters $U_{K,K'}(t)$ and $\Delta_{K,K'}(t)$. The detailed calculation of these parameters and the mean transition probabilities were described in Refs. [15, 21].

The evolution of the DNS along the variable R leads to the quasi-fission of the DNS. The quasi-fission rate Λ^{qf} can be estimated with the one-dimensional Kramers formula [26, 27]:

$$\Lambda^{qf}(\Theta(t)) = \frac{\omega}{2\pi\omega^{B_{qf}}} \left(\sqrt{\left(\frac{\Gamma}{2\hbar} \right)^2 + (\omega^{B_{qf}})^2} - \frac{\Gamma}{2\hbar} \right) \exp \left(-\frac{B_{qf}(A_1, A_2)}{\Theta(t)} \right). \tag{6}$$

Here the quasi-fission barrier is counted from the depth of the pocket of the interaction potential. The local temperature is given by the Fermi-gas expression $\Theta = \sqrt{\varepsilon^*/a}$ corresponding to the local excitation energy ε^* and level density parameter $a = A/12 \text{ MeV}^{-1}$. In Eq.(6) the frequency $\omega^{B_{qf}}$ is the frequency of the inverted harmonic oscillator approximating the interaction potential of two nuclei in R around the top of the quasi-fission barrier, and ω is the frequency of the harmonic oscillator approximating the potential in R around the bottom of the pocket. The quantity Γ , which denotes the double average width of the contributing single-particle states, determines the friction coefficients: $\gamma_{ii'} = \frac{\Gamma}{\hbar} \mu_{ii'}$, with $\mu_{ii'}$ being the inertia tensor. Here we use constant values $\Gamma = 2.8 \text{ MeV}$, $\hbar\omega^{B_{qf}} = 2.0 \text{ MeV}$ and $\hbar\omega = 3.0 \text{ MeV}$ for the following reactions. The Kramers formula is derived with the quasi-stationary condition of the temperature $\Theta(t) < B_{qf}(A_1, A_2)$. However, the numerical calculation in Ref. [27] indicated that Eq.(6) is also useful for the condition of $\Theta(t) > B_{qf}(A_1, A_2)$. In the reactions of synthesizing SHN, there is the possibility of the fission of the heavy fragment in the DNS. Because the fissility increases with the charge number of the nucleus, the fission of the heavy fragment can affect the quasi-fission and fusion when the DNS evolves towards larger mass asymmetry. The fission rate Λ^{fis} can also be treated with the

one-dimensional Kramers formula [26]

$$\Lambda^{fis}(\Theta(t)) = \frac{\omega_{g.s.}}{2\pi\omega_f} \left(\sqrt{\left(\frac{\Gamma_0}{2\hbar}\right)^2 + \omega_f^2} - \frac{\Gamma_0}{2\hbar} \right) \exp\left(-\frac{B_f(A_1, A_2)}{\Theta(t)}\right), \quad (7)$$

where the $\omega_{g.s.}$ and ω_f are the frequencies of the oscillators approximating the fission-path potential at the ground state and on the top of the fission barrier for nucleus A_1 or A_2 (larger fragment), respectively. Here, we take $\hbar\omega_{g.s.} = \hbar\omega_f = 1.0$ MeV, $\Gamma_0 = 2$ MeV. The fission barrier is calculated as the sum of a macroscopic part and the shell correction energy used in Refs. [15, 28]. The fission of the heavy fragment does not favor the diffusion of the system to a light fragment distribution. Therefore, it leads to a slight decrease of the fusion probability.

In the relaxation process of the relative motion, the DNS will be excited by the dissipation of the relative kinetic energy. The excited system opens a valence space $\Delta\varepsilon_K$ in fragment K ($K = 1, 2$), which has a symmetrical distribution around the Fermi surface. Only the particles in the states within this valence space are actively involved in excitation and transfer. The averages on these quantities are performed in the valence space:

$$\Delta\varepsilon_K = \sqrt{\frac{4\varepsilon_K^*}{g_K}}, \varepsilon_K^* = \varepsilon^* \frac{A_K}{A}, g_K = \frac{A_K}{12}, \quad (8)$$

where the ε^* is the local excitation energy of the DNS, which provides the excitation energy for the mean transition probability. There are $N_K = g_K \Delta\varepsilon_K$ valence states and $m_K = N_K/2$ valence nucleons in the valence space $\Delta\varepsilon_K$, which gives the dimension $d(m_1, m_2) = \binom{N_1}{m_1} \binom{N_2}{m_2}$. The local excitation energy is defined as

$$\varepsilon^* = E_x - (U(A_1, A_2) - U(A_P, A_T)). \quad (9)$$

Here the $U(A_1, A_2)$ and $U(A_P, A_T)$ are the driving potentials of fragments A_1, A_2 and fragments A_P, A_T (at the entrance point of the DNS), respectively. The detailed calculation of the driving potentials can be seen in Ref. [18]. The excitation energy E_x of the composite system is converted from the relative kinetic energy loss, which is related to the Coulomb barrier B [29] and determined for each initial relative angular momentum J by the parametrization method of the classical deflection function [24, 25]. So E_x is coupled with the relative angular momentum.

After reaching the reaction time in the evolution of $P(A_1, E_1, t)$, all those components on the left side of the B.G. (Businaro-Gallone) point contribute to the formation of the compound nucleus. The hindrance in the diffusion process by nucleon transfer to form the compound nucleus is the inner fusion barrier B_{fus} , which is defined as the difference of the driving potential at the

B.G. point and at the entrance position. Nucleon transfers to more symmetric fragments undergo quasi-fission. The formation probability of the compound nucleus at the Coulomb barrier B (here a barrier distribution $f(B)$ is considered) and angular momentum J is given by

$$P_{CN}(E_{c.m.}, J, B) = \sum_{A_1=1}^{A_{BG}} P(A_1, E_1, \tau_{int}(E_{c.m.}, J, B)). \quad (10)$$

Here the interaction time $\tau_{int}(E_{c.m.}, J, B)$ is obtained using the deflection function method [30], which means the time duration for nucleon transfer from the capture stage to the formation of the complete fused system with the order of 10^{-20} s. We obtain the fusion probability as

$$P_{CN}(E_{c.m.}, J) = \int f(B) P_{CN}(E_{c.m.}, J, B) dB, \quad (11)$$

where the barrier distribution function is taken in asymmetric Gaussian form [13, 15]. So the fusion cross section is written as

$$\sigma_{fus}(E_{c.m.}) = \frac{\pi \hbar^2}{2\mu E_{c.m.}} \sum_{J=0}^{\infty} (2J+1) T(E_{c.m.}, J) P_{CN}(E_{c.m.}, J). \quad (12)$$

The survival probability of the excited compound nucleus cooled by the neutron evaporation in competition with fission is expressed as follows:

$$W_{sur}(E_{CN}^*, x, J) = P(E_{CN}^*, x, J) \prod_{i=1}^x \left(\frac{\Gamma_n(E_i^*, J)}{\Gamma_n(E_i^*, J) + \Gamma_f(E_i^*, J)} \right)_i, \quad (13)$$

where the E_{CN}^*, J are the excitation energy and the spin of the compound nucleus, respectively. The E_i^* is the excitation energy before evaporating the i th neutron, which has the relation

$$E_{i+1}^* = E_i^* - B_i^n - 2T_i, \quad (14)$$

with the initial condition $E_1^* = E_{CN}^*$. The energy B_i^n is the separation energy of the i th neutron. The nuclear temperature T_i is given by $E_i^* = aT_i^2 - T_i$ with the level density parameter a . $P(E_{CN}^*, x, J)$ is the realization probability of emitting x neutrons. The widths of neutron evaporation and fission are calculated using the statistical model. The details can be found in Ref. [15]. The level density is expressed by the back-shifted Bethe formula [31] with the spin cut-off model as

$$\rho(E^*, J) = K_{rot} K_{vib} \frac{2J+1}{24\sqrt{2}\sigma^3} a^{-1/4} (E^* - \Delta)^{-5/4} \exp[2\sqrt{a(E^* - \Delta)}] \exp\left[-\frac{(J+1/2)^2}{2\sigma^2}\right], \quad (15)$$

where the K_{rot} and K_{vib} are the coefficients of the rotational and vibrational enhancements. The pairing energy is given by

$$\Delta = \chi \frac{12}{\sqrt{A}} \quad (16)$$

in MeV($\chi=-1, 0$ and 1 for odd-odd, odd-even and even-even nuclei, respectively). The spin cut-off parameter is calculated by the formula:

$$\sigma^2 = T\zeta_{r.b}/\hbar^2, \quad (17)$$

where the rigid-body moment of inertia has the relation $\zeta_{r.b} = 0.4MR^2$ with the mass M and the radius R of the nucleus. The level density parameter is related to the shell correction energy $E_{sh}(Z, N)$ and the excitation energy E^* of the nucleus as

$$a(E^*, Z, N) = \tilde{a}(A)[1 + E_{sh}(Z, N)f(E^* - \Delta)/(E^* - \Delta)]. \quad (18)$$

Here, $\tilde{a}(A) = \alpha A + \beta A^{2/3}b_s$ is the asymptotic Fermi-gas value of the level density parameter at high excitation energy. The shell damping factor is given by

$$f(E^*) = 1 - \exp(-\gamma E^*) \quad (19)$$

with $\gamma = \tilde{a}/(\epsilon A^{4/3})$. All the used parameters are listed in Table 1. In Fig.1 we give the level density parameters of different nuclides at the ground state calculated by using Eq.(18) and compared them with two empirical formulas $a(A) = A/8$, and $A/12$. It can be seen that the strong shell effects appear in the level density.

With this procedure introduced above, we calculated the angular momentum dependence of the capture, fusion and survival probabilities as shown in Fig.2 for the reaction $^{48}\text{Ca}+^{208}\text{Pb}$ at incident energies 172.36 MeV and 192.36 MeV, respectively. The values of the three stages decrease obviously with increasing the relative angular momentum. So in the following estimation of the production cross sections, we cut off the maximal angular momentum at $J_{max} = 30$, which is taken as the same value that used in the cold fusion reactions [18].

3 Results and discussions

3.1 Fusion-fission reactions and quasi-fission mass yields

As a test of the parameters for the estimation of the transmission of two colliding nuclei and the de-excitation of the thermal compound nucleus, we analyzed the fusion-fission reactions for the selected systems shown in Fig.3 assuming $P_{CN} = 1$. The capture and evaporation residue cross sections are compared with the available experimental data [32, 33, 34, 35]. For these systems the quasi-fission does not dominate in the sub-barrier region, which also means that $P_{CN} \sim 1$.

The evaporation residues are mainly determined through the capture of the light projectile by the target nucleus and the survival probabilities of the formed compound nucleus. The experimental data can be reproduced rather well within the error bars. Some discrepancies may come from the quasi-fission in the above barrier region and from the input quantities, such as the neutron separation energy, shell correction and mass. The rotational and the vibrational enhancement in the level density can also affect the survival probabilities of the excited compound nucleus [36]. Here we take unity for both coefficients as shown in Table 1 because the height of the fission barrier is also sensitive to the survival of the compound nucleus by fitting the experimental evaporation residue excitation functions in the fusion-fission reactions.

Since the electrostatic energy of the composite systems formed by two heavy colliding nuclei is very large, so although the two nuclei may be captured by the nuclear potential, they almost always separate after mass transfer from the heavier nucleus to the lighter one rather fusing. This process is called quasi-fission [37, 38], which is the main feature in the massive fusion reactions and can inhibit fusion by several degree of freedom. Recently, experiment has performed nice works by measuring the quasi-fission and fusion-fission mass yields [39]. In the DNS model, the quasi-fission mass yields are expressed as [26]

$$Y_{q-f}(A_1) = \sum_{J=0}^{J_{max}} \int_0^{\tau_{int}} P(A_1, E_1, t) \Lambda^{qf}(\Theta(t)) dt. \quad (20)$$

In Fig.4 we show a comparison of the calculated quasi-fission mass yields and the experimental data for the two ^{48}Ca induced reaction systems. The trends of the distribution can be reproduced by the DNS model. At the domain of the medium-mass fragments $A_1=A_{CN}/2-30 \sim A_{CN}/2+30$, The experimental data are higher than the calculated values, which may be come from the contribution of the fusion-fission fragments.

3.2 Evaporation residue cross sections

The evaporation residues observed in laboratories by the consecutive α decay are mainly produced by the complete fusion reactions, in which the fusion dynamics and the structure properties of the compound nucleus affect their production. Within the framework of the DNS model, we calculated the evaporation residue cross sections producing SHN $Z=110, 112, 113, 115$ with ^{232}Th , ^{238}U , ^{237}Np and ^{243}Am targets in the ^{48}Ca induced reactions as shown in Fig.5, and compared them with the Dubna data [7, 40, 41] as well as with the recent GSI data [42] for ^{238}U targets in the $3n$ channel. Compared with the Dubna data for the system $^{48}\text{Ca}+^{238}\text{U}$, the GSI results show that the formation cross sections in the $3n$ channel have a slight decrease at the same excitation energy, which is in

a good agreement with our calculated results. The calculations were carried out before getting the experimental data [41] for the reaction $^{48}\text{Ca}+^{237}\text{Np}$, and a good agreement with the data is also found [43]. The excitation energy of the compound nucleus is obtained by $E_{CN}^* = E_{c.m.} + Q$, where the $E_{c.m.}$ is the incident energy in the center-of-mass system. The Q value is given by $Q = \Delta M_P + \Delta M_T - \Delta M_C$, and the corresponding mass excesses ΔM_i ($i = P, T, C$) are taken the data from Ref. [44] for the projectile, target and compound nucleus denoted with the symbols P , T and C , respectively. Usually, the neutron-rich projectile-target combinations are in favor of synthesizing SHN experimentally, which can enhance the survival probability W_{sur} in Eq.(1) of the formed compound nucleus because of the smaller neutron separation energy. Differently to the cold fusion reactions [18], the maximal production cross sections from Ds to 115 especially in the 2n-5n channels are not changed much although the heavier SHNs are synthesized. Within the error bars the experimental data can be reproduced rather well. With the same procedure, we analyzed the evaporation residue excitation functions with targets $^{242,244}\text{Pu}$ and $^{245,248}\text{Cm}$ that are used to synthesize the superheavy elements $Z=114$ and 116 in Dubna [40, 45] (Fig.6). Our calculations show that the target ^{244}Pu has a larger production cross section than ^{242}Pu because of the larger survival probability. In Fig.7 we also calculated the evaporation residue excitation functions to synthesize superheavy elements $Z=117-120$ using the actinide isotopes with longer half-lives ^{247}Bk , ^{249}Cf , ^{254}Es and ^{257}Fm . The 3n evaporation channel with an excitation energy of the formed compound nucleus around 30 MeV is favorable to produce SHN with $Z \geq 117$ by using the actinide targets. Within the error bars, the positions of the maximal production cross sections are in good agreement with the available experimental results. Similar calculation of the evaporation residue excitation functions was also reported in Ref. [46]. The spectrum form of evaporating neutrons is mainly determined by the survival probability, in which the neutron separation energy and the shell correction play a very important role in the determination of the value. We considered the angular momentum influence in the calculation of the level density, but did not include it in the estimation of the fission barrier of the thermal compound nucleus. As pointed out in section 1, the fission barrier of SHN decreases rapidly with increasing excitation energy of the compound nucleus, where the rotation of the system affects the height of the barrier and also influences other crucial quantities such as the level density etc.

In Fig.8 we show a comparison of the calculated maximal production cross sections of superheavy elements $Z=102-120$ in the cold fusion reactions by evaporating one neutron, in the ^{48}Ca induced reactions with actinide targets by evaporating three neutrons, and the experimental data [1, 2, 4, 47]. The production cross sections decrease rapidly with increasing the charge number of

the synthesized compound nucleus in the cold fusion reactions, such as from $0.2 \mu\text{b}$ for the reaction $^{48}\text{Ca}+^{208}\text{Pb}$ to 1 pb for $^{70}\text{Zn}+^{208}\text{Pb}$, and even below 0.1 pb for synthesizing $Z\geq 113$ [18]. It seems to be difficult to synthesize superheavy elements $Z\geq 113$ in the cold fusion reactions at the present facilities. The calculated results show that the ^{48}Ca induced reactions have smaller production cross sections with ^{232}Th target, but are in favor of synthesizing heavier SHN ($Z\geq 113$) because of the larger cross sections. The experimental data also give such trends. In the DNS concept, the inner fusion barrier increases with reducing mass asymmetry in the cold fusion reactions, which leads to a decrease of the formation probability of the compound nucleus. However, the ^{48}Ca induced reactions have not such increase of the inner fusion barrier for synthesizing heavier SHN. Because of the larger transmission and the higher fusion probability, we obtain larger production cross sections for synthesizing SHN ($Z\geq 113$) in the ^{48}Ca induced reactions although these reactions have the smaller survival probability than those in the cold fusion reactions. It is still a good way to synthesize heavier SHN by using the ^{48}Ca induced reactions. Of course, further experimental data are anticipated to be obtained in the future. However, the actinide targets are difficult to be handled in experiments synthesizing heavier SHN.

3.3 Isotopic dependence of the production cross sections

Recent experimental data show that the production cross sections of the SHN depend on the isotopic combination of the target and projectile in the ^{48}Ca induced fusion reactions. For example, the maximal cross section in the $3n$ channel is $3.7\pm_{1.8}^{3.6} \text{ pb}$ for the reaction $^{48}\text{Ca}+^{245}\text{Cm}$ at the excitation energy 37.9 MeV ; however, it is 1.2 pb for the reaction $^{48}\text{Ca}+^{248}\text{Cm}$ although the later is a neutron-rich target [8, 40]. The isotopic trends of the production cross sections were also observed and investigated in cold fusion reactions [48, 18]. Further investigations on the isotopic trends in the ^{48}Ca induced reactions are very necessary for predicting the optimal combinations, excitation energies (incident energies) and evaporation channels in the synthesis of SHN. In Fig.9 we show the calculated isotopic trends in producing superheavy elements $Z=110, 112$ with the isotopic actinides Th and U in the $3n$ channels, and compare them with the available experimental data performed in Dubna [40] (squares with error bars) and at GSI [42] (circles with error bars). The results show that the targets ^{230}Th in the $4n$ channel and $^{235,238}\text{U}$ in the $3n$ channel have the largest cross sections. The isotopic trends in synthesizing $Z=113-116$ with the actinide targets Np, Pu, Am and Cm are also calculated systematically, and compared with the existing data measured in Dubna [7, 40, 45] and the results of Adamian et al. [49] for the Pu isotopes as shown

in Fig.10 and Fig.11. The isotopes ^{237}Np , ^{241}Pu , $^{242,243}\text{Am}$ and $^{245,247}\text{Cm}$ in the 3n channels, and ^{244}Pu in the 4n channel as well as the isotope ^{250}Cm are suitable for synthesizing SHN. Except for the ^{244}Pu , our calculated cross sections are smaller than the ones of the Adamian et al. In the DNS model, the isotopic dependence of the production cross sections is mainly determined by both the fusion and survival probabilities. Of course, the transmission probability of two colliding nuclei can also be affected since the isotopes have initial quadrupole deformations. With the same procedure, we analyzed the dependence of the production cross sections on the isotopes Bk and Cf in the 3n channels for synthesizing the superheavy elements $Z=117$, 118 and compared them with the available experimental data [8] shown in Fig.12. The results show that the targets $^{248,249}\text{Bk}$ and $^{251,252}\text{Cf}$ are favorable for synthesizing the superheavy elements $Z=117$ and 118. The corresponding excitation energies are also given in the figures.

In Fig.13 we show the dependence of the inner fusion barrier, the fission barrier of the compound nucleus, and the neutron separation energies of evaporating 3n and 4n on the mass numbers of the isotopic targets Cm in the ^{48}Ca induced reactions. It is obvious that the combinations with the isotopes $^{245,247}\text{Cm}$ have smaller inner fusion barriers, higher fission barriers and smaller 3n separation energies, which result in larger production cross sections producing the superheavy element $Z=116$. Although the lower fission barrier for the isotope ^{250}Cm , it gives the smaller inner fusion barrier and neutron separation energies, which also leads to the larger cross sections in the 3n and 4n channels as shown in Fig.11. The shell correction and the neutron separation energies are taken from Ref. [44]. When the neutron number of the target increases, the DNS gets more asymmetrical and the fusion probability increases if the DNS does not consist of more stable nuclei (such as magic nuclei) because of a smaller inner fusion barrier. A smaller neutron separation energy and a larger shell correction lead to a larger survival probability. The compound nucleus with closed neutron shells has a larger shell correction energy and a larger neutron separation energy. The neutron-rich actinide target has larger fusion and survival probabilities due to the larger asymmetric initial combinations and smaller neutron separation energies. But such actinide isotopes are usually unstable with smaller half-lives. With the establishment of the high intensity radioactive-beam facilities, the neutron-rich SHN may be synthesized experimentally, which approaches the island of stability.

3.4 ^{238}U based reactions

The uranium is the heaviest element existing in the nature. It has a larger mass asymmetry constructed as a target in the fusion reactions with the various neutron-rich light projectiles. The isotope ^{238}U is the neutron-richest nucleus in the U isotopes and often chosen as the target for synthesizing SHN. In Fig.14 we give evaporation residue excitation functions of the reactions ^{40}Ar , ^{50}Ti , ^{54}Cr , $^{64}\text{Ni}+^{238}\text{U}$ in the 2n-5n channels. The results show that the 4n channel in the reaction $^{40}\text{Ar}+^{238}\text{U}$ has the larger cross sections with 2.1 pb at an excitation energy 42 MeV. This reaction is being used to synthesize the superheavy nucleus Ds with HIRFL accelerator at Institute of Modern Physics in Lanzhou. The reactions ^{50}Ti , ^{54}Cr , $^{64}\text{Ni}+^{238}\text{U}$ lead to the cross section smaller than 0.1 pb. The isotopic trends based on the U isotopes are also investigated using the DNS model as shown in Fig.15. Calculations show that the isotopes ^{235}U and ^{238}U are favorable in producing SHN. The cross sections are reduced with increasing the mass numbers of the projectiles. Other reaction mechanisms to synthesize SHN have to be investigated with theoretical models, such as the massive transfer reactions, and the complete fusion reactions induced by weakly bound nuclei. Work in these directions is in progress within the framework of the DNS model.

4 Conclusions

Using the DNS model, we systematically investigated the production of superheavy residues in fusion-evaporation reactions, in which the nucleon transfer leading to the formation of the superheavy compound nucleus is described with a set of microscopically derived master equations that are solved numerically and include the quasi-fission of the DNS and the fission of the heavy fragments. The fusion dynamics and the evaporation residue excitation functions in the ^{48}Ca fusion reactions are systematically investigated. The calculated results are in good agreement with the available experimental data within the error bars. Isotopic trends in the production of superheavy elements are analyzed. It is shown that the isotopes $^{235,238}\text{U}$, ^{237}Np , $^{241,244}\text{Pu}$, ^{242}Am and $^{245,247,250}\text{Cm}$, $^{248,249}\text{Bk}$ and $^{251,252}\text{Cf}$ in the 3n channels, and ^{230}Th , ^{244}Pu , $^{248,250}\text{Cm}$ in the 4n channels are favorable for producing the superheavy elements Z=110, 112 and 113-118, respectively. The evaporation residue excitation functions of the reactions ^{40}Ar , ^{50}Ti , ^{54}Cr , $^{64}\text{Ni}+^{238}\text{U}$ in the 2n-5n channels and the isotopic trends with ^{40}Ar , ^{48}Ca , ^{50}Ti , ^{54}Cr , ^{58}Fe and ^{64}Ni bombarding U isotopes are also studied.

5 Acknowledgement

One of us (Z.-Q. Feng) is grateful to Prof. H. Feldmeier, Dr. G.G. Adamian and Dr. N.V. Antonenko for fruitful discussions and help, and also thanks the hospitality during his stay in GSI. This work was supported by the National Natural Science Foundation of China under Grant No. 10805061, the special foundation of the president fellowship, the west doctoral project of Chinese Academy of Sciences, and major state basic research development program under Grant No. 2007CB815000.

References

- [1] S. Hofmann and G. Münzenberg, *Rev. Mod. Phys.* 72 (2000) 733; S. Hofmann, *Rep. Prog. Phys.* 61 (1998) 639.
- [2] Yu.Ts. Oganessian, *J. Phys. G* 34 (2007) R165; *Nucl. Phys. A* 787 (2007) 343c.
- [3] Yu.Ts. Oganessian, A.S. Iljnov, A.G. Demin, et al., *Nucl. Phys. A* 239 (1975) 353; *Nucl. Phys. A* 239 (1975) 157.
- [4] G. Münzenberg, *J. Phys. G* 25 (1999) 717.
- [5] K. Morita, K. Morimoto, D. Kaji, et al., *J. Phys. Soc. Jpn.* 73 (2004) 2593.
- [6] Yu.Ts. Oganessian, A.G. Demin, A.S. Iljnov, et al., *Nature* 400 (1999) 242; Yu.Ts. Oganessian, V.K. Utyonkov, Yu.V. Lobanov, et al., *Phys. Rev. C* 62 (2000) 041604(R).
- [7] Yu.Ts. Oganessian, V.K. Utyonkov, Yu.V. Lobanov, et al., *Phys. Rev. C* 69 (2004) 021601(R).
- [8] Yu.Ts. Oganessian, V.K. Utyonkov, Yu.V. Lobanov, et al., *Phys. Rev. C* 74 (2006) 044602.
- [9] Z.G. Gan, Z. Qin, H.M. Fan, et al., *Eur. Phys. J. A* 10 (2001) 21; Z.G. Gan, J.S. Guo, X.L. Wu, et al., *Eur. Phys. J. A* 20 (2004) 385.
- [10] W.J. Swiatecki, *Prog. Part. Nucl. Phys.* 4 (1980) 383.
- [11] S. Bjornholm and W.J. Swiatecki, *Nucl. Phys. A* 391 (1982) 471.
- [12] Y. Aritomo, T. Wada, M. Ohta, and Y. Abe, *Phys. Rev. C* 59 (1999) 796.

- [13] V.I. Zagrebaev, Phys. Rev. C 64 (2001) 034606; V.I. Zagrebaev, Y. Aritomo, M.G. Itkis, Yu.Ts. Oganessian, and M. Ohta, Phys. Rev. C 65 (2001) 014607.
- [14] G.G. Adamian, N.V. Antonenko, W. Scheid et al., Nucl. Phys. A 627 (1997) 361; Nucl. Phys. A 633 (1998) 409.
- [15] Z.Q. Feng, G.M. Jin, F. Fu, and J.Q. Li, Nucl. Phys. A 771 (2006) 50.
- [16] N. Wang, Z.X. Li, X.Z. Wu, et al., Phys. Rev. C 69 (2004) 034608; N. Wang, Z.X. Li, X.Z. Wu, and E. G. Zhao, Mod. Phys. Lett. A 20 (2005) 2619.
- [17] Z.Q. Feng, G.M. Jin and F.S. Zhang, Nucl. Phys. A 802 (2008) 91; Z.Q. Feng, F.S. Zhang, G.M. Jin, and X. Huang, Nucl. Phys. A 750 (2005) 232; Z.Q. Feng, G.M. Jin, F.S. Zhang, et al., Chin. Phys. Lett. 22 (2005) 3040.
- [18] Z.Q. Feng, G.M. Jin, J.Q. Li, and W. Scheid, Phys. Rev. C 76 (2007) 044606.
- [19] V. V. Volkov, Phys. Rep. 44 (1978) 93.
- [20] P. Reiter, T.L. Khoo, T. Lauritsen, et al., Phys. Rev. Lett. 84 (2000) 3542.
- [21] W. Li, N. Wang, J. Li, et al., Eur. Phys. Lett. 64 (2003) 750; J. Phys. G 32 (2006) 1143.
- [22] A. Diaz-Torres, G.G. Adamian, N.V. Antonenko, and W. Scheid, Phys. Rev. C 64 (2001) 024604; A. Diaz-Torres, Phys. Rev. C 74 (2006) 064601.
- [23] W. Nörenberg, Z. Phys. A 274 (1975) 241; S. Ayik, B. Schürmann and Nörenberg, Z. Phys. A 277 (1976) 299.
- [24] G. Wolschin and W. Nörenberg, Z. Phys. A 284 (1978) 209.
- [25] J.Q. Li, X.T. Tang, G. Wolschin, Phys. Lett. B 105 (1981) 107.
- [26] G.G. Adamian, N.V. Antonenko and W. Scheid, Phys. Rev. C 68 (2003) 034601.
- [27] P. Grangé, Li Jun-Qing and H. A. Weidenmüller, Phys. Rev. C 27 (1983) 2063.
- [28] G.G. Adamian, N.V. Antonenko, S.P. Ivanova, and W. Scheid, Phys. Rev. C 62 (2000) 064303.
- [29] Z.Q. Feng, G.M. Jin, F. Fu, and J. Q. Li, High Ener. Phys. Nucl. Phys., 31 (2007) 366.
- [30] J.Q. Li, G. Wolschin, Phys. Rev. C 27 (1983) 590.

- [31] H. Bethe, Phys. Rev. 50 (1936) 332; Rev. Mod. Phys. 9 (1937) 69.
- [32] E.V. Prokhorova, A.A. Bogachev, M.G. Itkis, et al., Nucl. Phys. A 802 (2008) 45.
- [33] M. Dasgupta and D.J. Hinde, Nucl. Phys. A 734 (2004) 148.
- [34] K. Nishio, H. Ikezoe, Y. Nagame, et al., Phys. Rev. Lett. 93 (2004) 162701.
- [35] J.M. Gates, M.A. Garcia, K.E. Gregorich, et al., Phys. Rev. C 77 (2008) 034603.
- [36] A.R. Junghans, M.de Jong, H.-G. Clerc, et al., Nucl. Phys. A 629 (1998) 635.
- [37] B.B. Back, Phys. Rev. C 31 (1985) 2104.
- [38] J. Toke, R. Bock, G.X. Dai, et al., Nucl. Phys. A 440 (1985) 327.
- [39] M.G. Itkis, J. Äystö, S. Beghini, et al., Nucl. Phys. A 734 (2004) 136.
- [40] Yu.Ts. Oganessian, V.K. Utyonkov, Yu.V. Lobanov, et al., Phys. Rev. C 70 (2004) 064609.
- [41] Yu.Ts. Oganessian, V.K. Utyonkov, Yu.V. Lobanov, et al., Phys. Rev. C 76 (2007) 011601(R).
- [42] S. Hofmann, D. Ackermann, S. Antalic, et al., Eur. Phys. J. A 32 (2007) 251.
- [43] Z.Q. Feng, PhD thesis, Institute of Modern Physics, Chinese Academy of Sciences, 2007.
- [44] P. Möller et al., At. Data Nucl. Data Tables 59 (1995) 185.
- [45] Yu.Ts. Oganessian, V.K. Utyonkov, Yu.V. Lobanov, et al., Phys. Rev. C 69 (2004) 054607.
- [46] V.I. Zagrebaev, Nucl. Phys. A 734 (2004) 164.
- [47] K.E. Gregorich, T.N. Ginter, W. Loveland, et al., Eur. Phys. J. A 18 (2003) 633.
- [48] S. Hofmann, V. Ninov, F.P. Heßberger, et al., Z. Phys. A 350 (1995) 277.
- [49] G. G. Adamian, N. V. Antonenko, and W. Scheid, Phys. Rev. C 69 (2004) 014607.

Table 1: Parameters used in the calculation of the level density.

K_{rot}	K_{vib}	b_s	α	β	ϵ
1	1	1	0.114	0.098	0.4

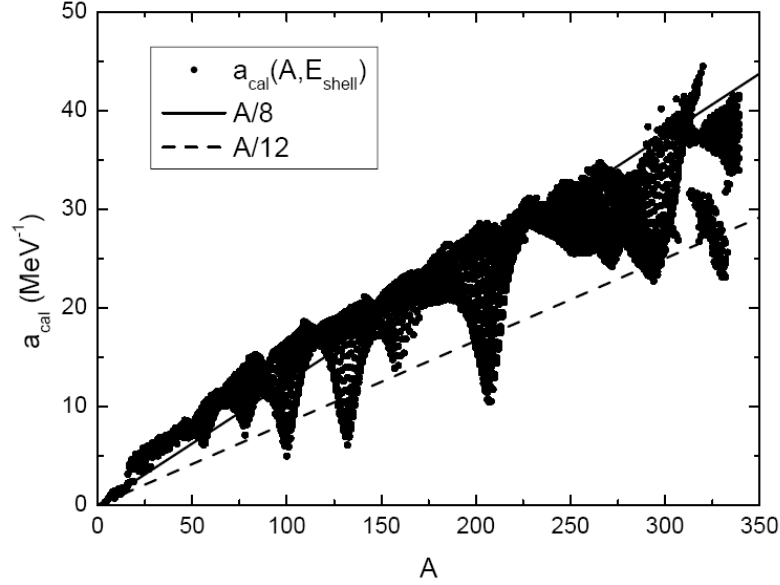


Figure 1: Calculated values of the level density parameters as a function of the atomic mass.

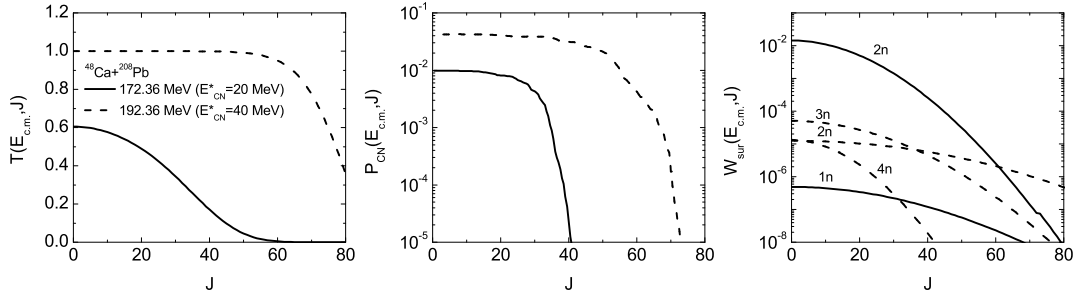


Figure 2: Calculated capture, fusion and survival probabilities as functions of the relative angular momenta in the reaction $^{48}\text{Ca}+^{208}\text{Pb}$ at excitation energies of the compound nucleus of 20 MeV and 40 MeV, respectively.

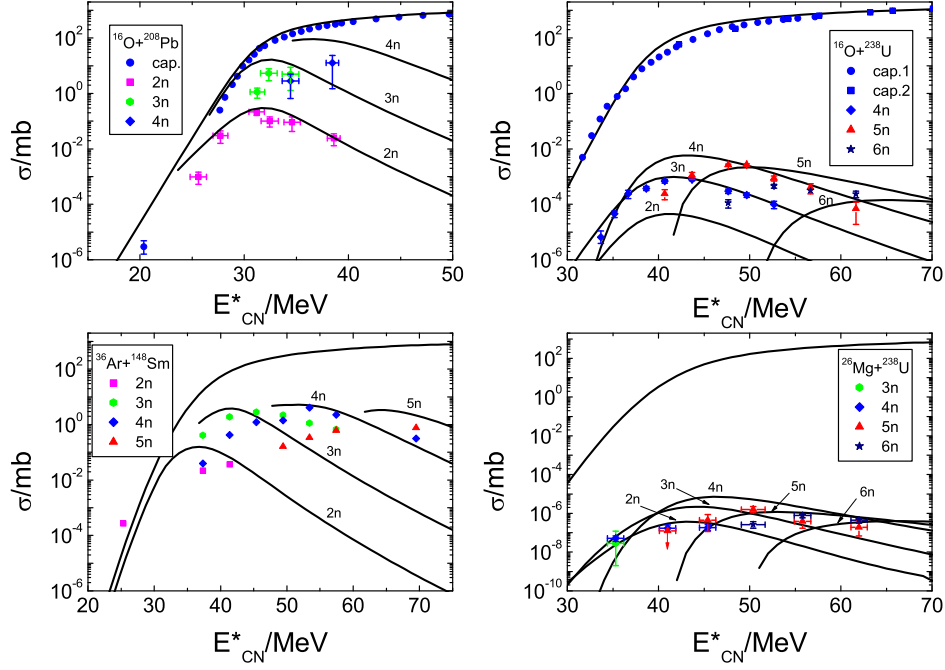


Figure 3: Comparison of the calculated fusion-fission excitation functions and the available experimental data for the reactions $^{16}\text{O}+^{208}\text{Pb}$, $^{16}\text{O}+^{238}\text{U}$, $^{36}\text{Ar}+^{148}\text{Sm}$ and $^{26}\text{Mg}+^{238}\text{U}$.

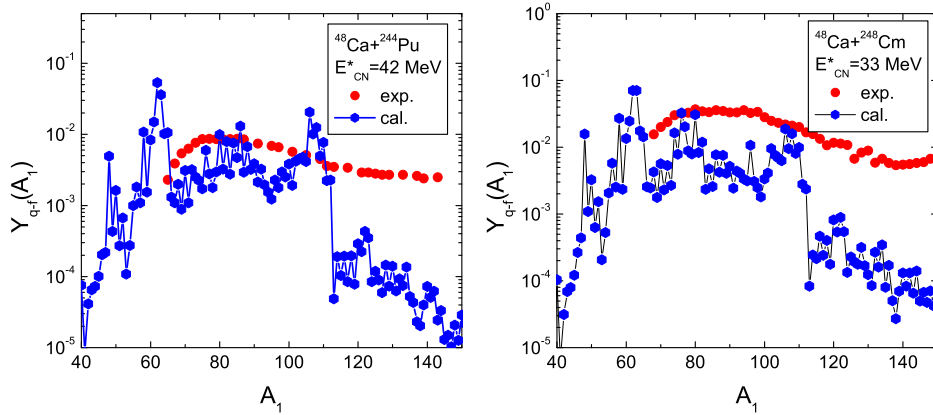


Figure 4: Calculated quasi-fission mass yields for the reactions $^{48}\text{Ca}+^{244}\text{Pu}$ and $^{48}\text{Ca}+^{248}\text{Cm}$ at excitation energies of the compound nuclei 42 MeV and 33 MeV, respectively, and compared them with the available experimental data [39].

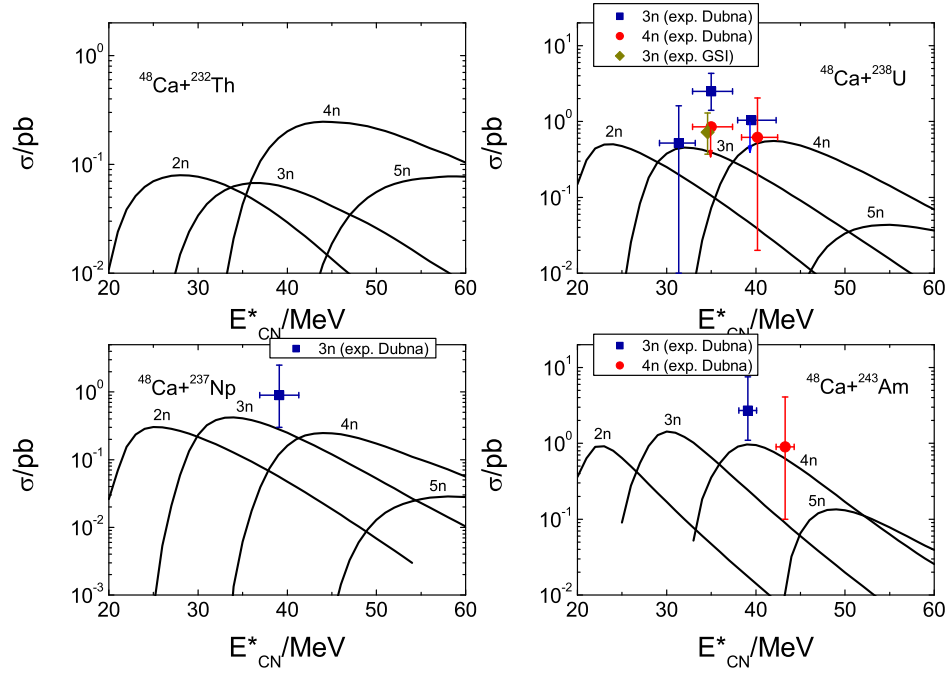


Figure 5: The calculated evaporation residue excitation functions with ^{232}Th , ^{238}U , ^{237}Np and ^{243}Am targets in ^{48}Ca induced reactions, and compared with the available experimental data [7, 40, 41].

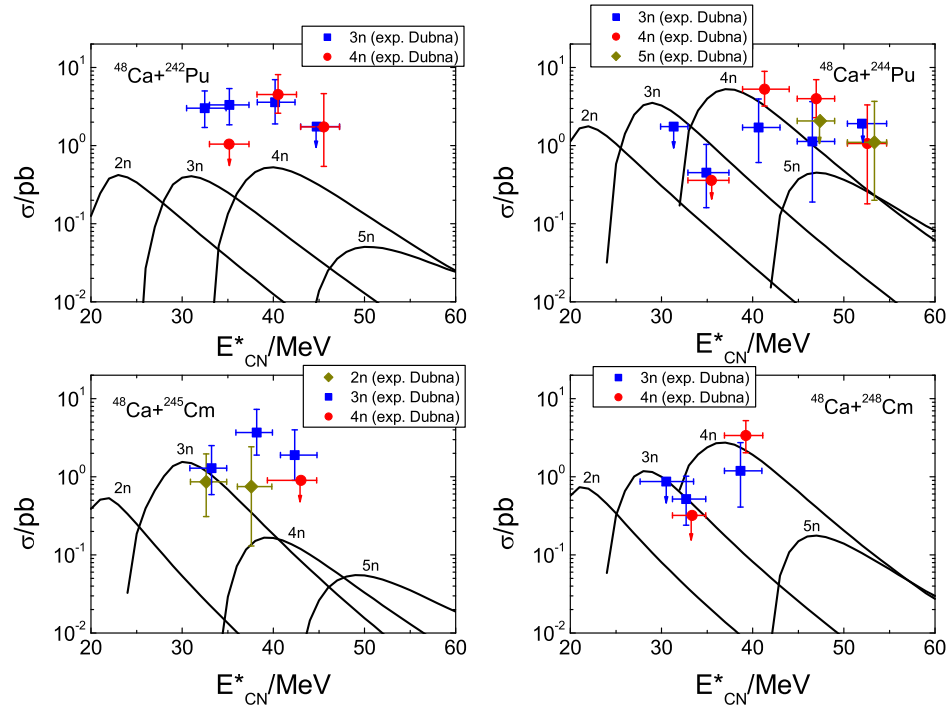


Figure 6: The same as in Fig.5, but for the targets $^{242,244}\text{Pu}$ and $^{245,248}\text{Cm}$ to produce superheavy elements $Z=114$ and 116 .

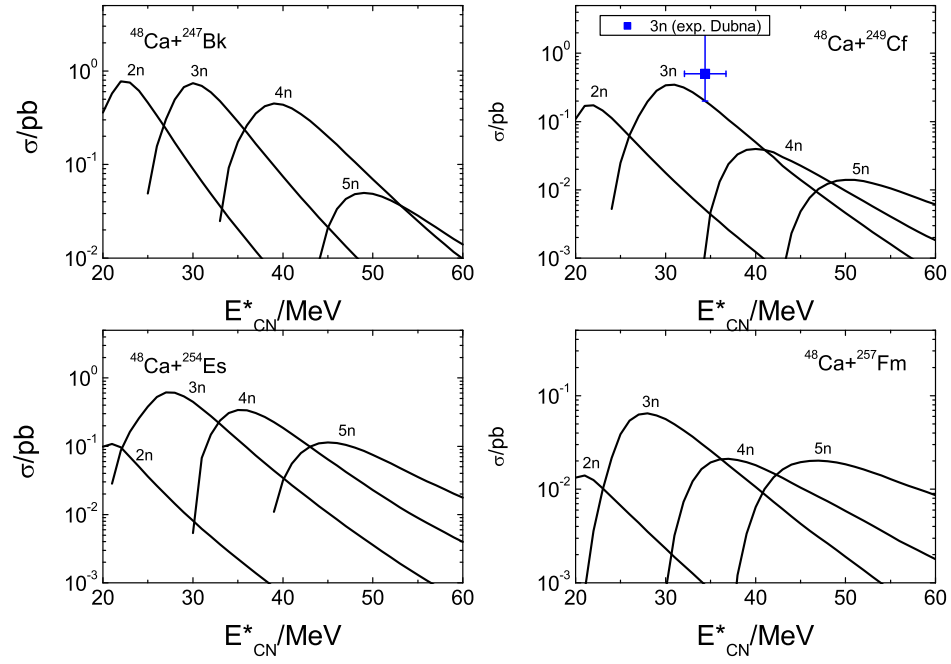


Figure 7: The same as in Fig.5, but for the targets ^{247}Bk , ^{249}Cf , ^{254}Es and ^{257}Fm to synthesize superheavy elements $Z=117-120$.

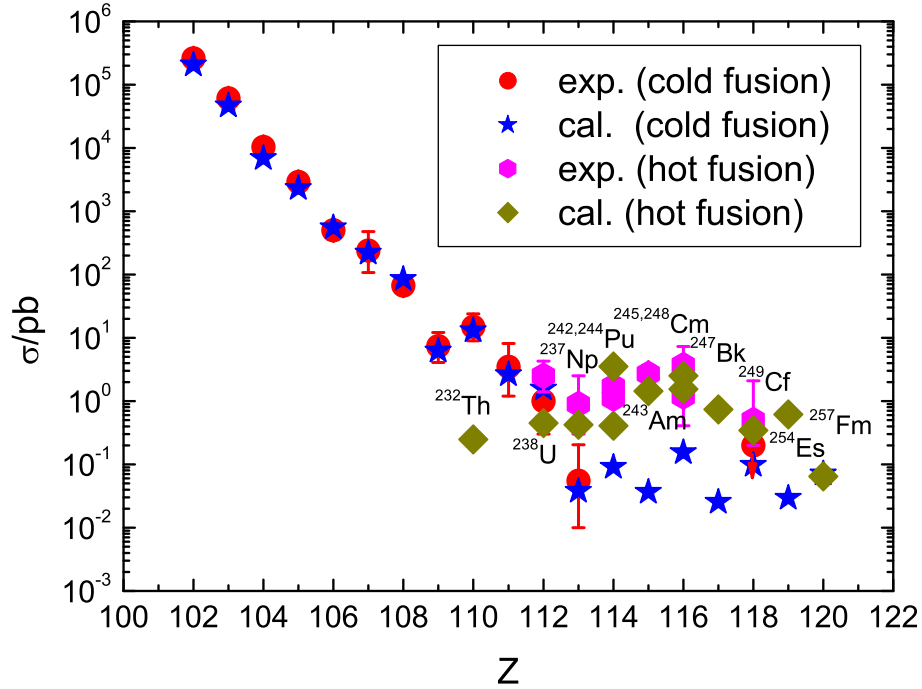


Figure 8: Maximal production cross sections of superheavy elements $Z=102-120$ in cold fusion reactions based on ^{208}Pb and ^{209}Bi targets with projectile nuclei ^{48}Ca , ^{50}Ti , ^{54}Cr , ^{58}Fe , ^{64}Ni , ^{70}Zn , ^{76}Ge , ^{82}Se , ^{86}Kr and ^{88}Sr , in ^{48}Ca induced reactions with actinide targets by evaporating 3 neutrons, in comparison with available experimental data [1, 2, 4, 47].

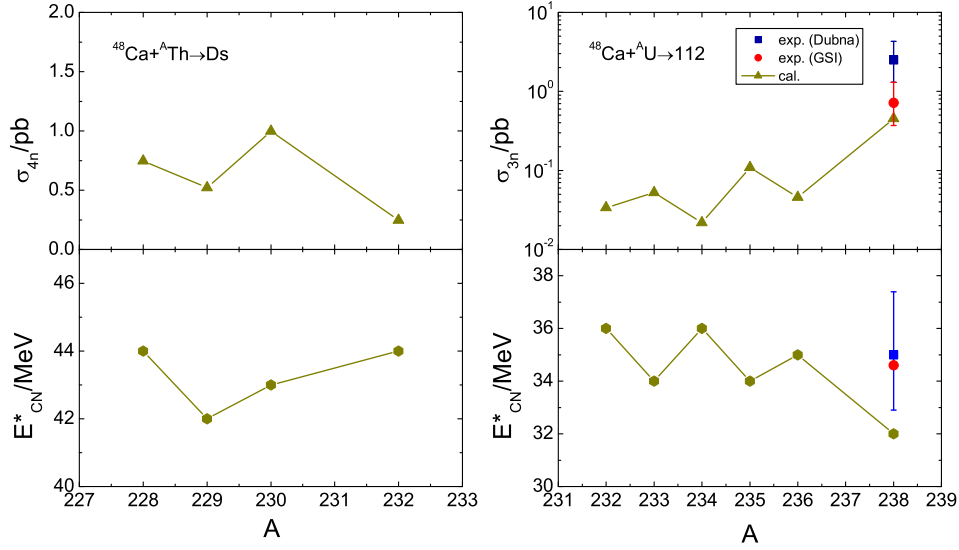


Figure 9: Isotopic dependence of the calculated maximal production cross sections in the 3n evaporation channel and the corresponding excitation energies in the synthesis of superheavy elements $Z=110$ and 112 for the reactions $^{48}\text{Ca} + ^A\text{Th}$ and $^{48}\text{Ca} + ^A\text{U}$, and compared with the experimental data [40, 42].

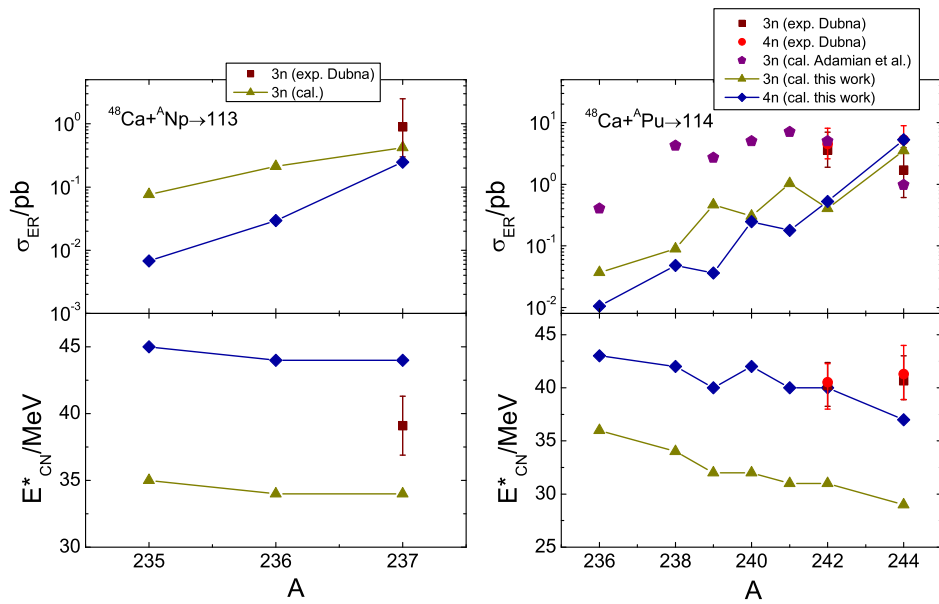


Figure 10: The same as in Fig.9, but for isotopic targets Np and Pu to produce superheavy elements $Z=113$ and 114.

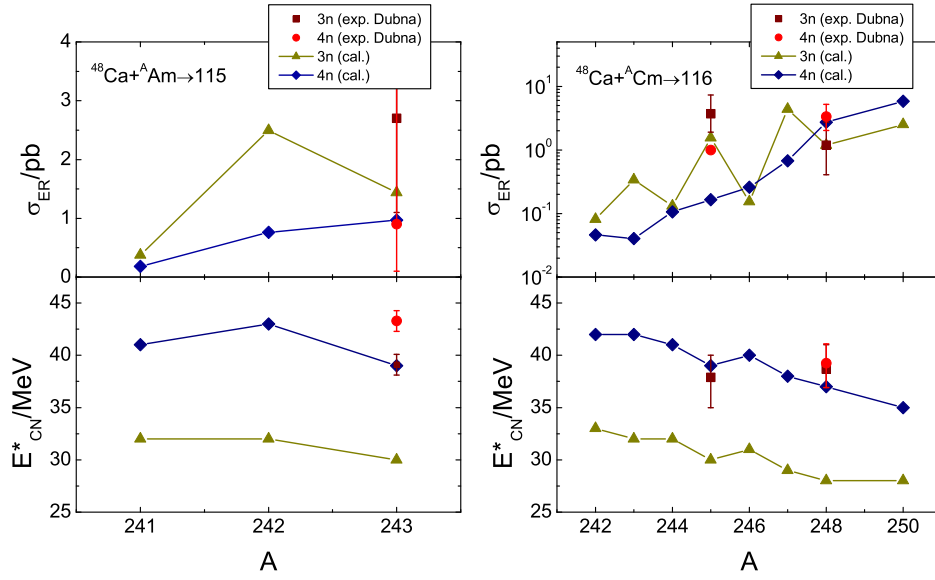


Figure 11: The same as in Fig.9, but for isotopic targets Am and Cm to synthesize superheavy elements $Z=115$ and 116 in $3n$ and $4n$ channels.

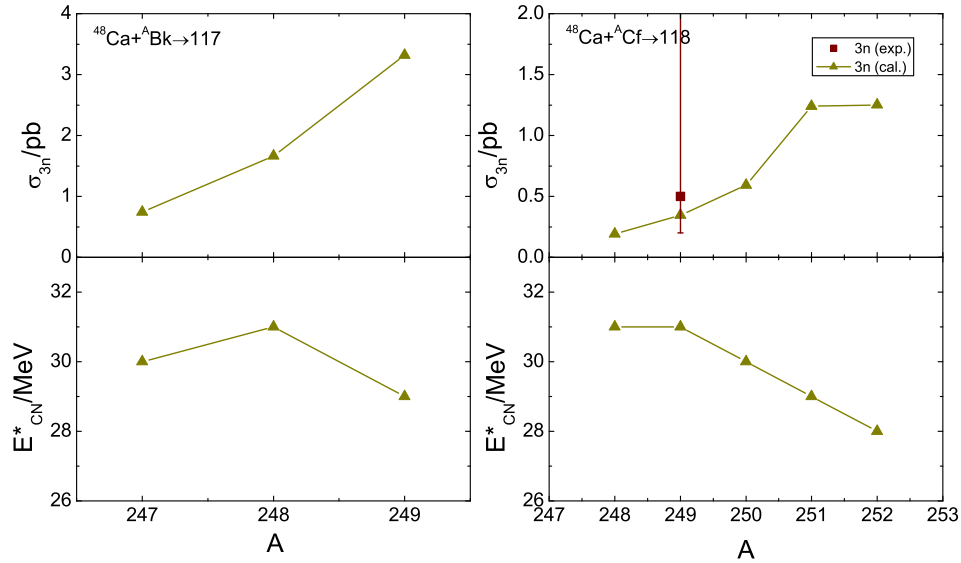


Figure 12: The same as in Fig.9, but for isotopes Bk and Cf in ^{48}Ca induced reactions.

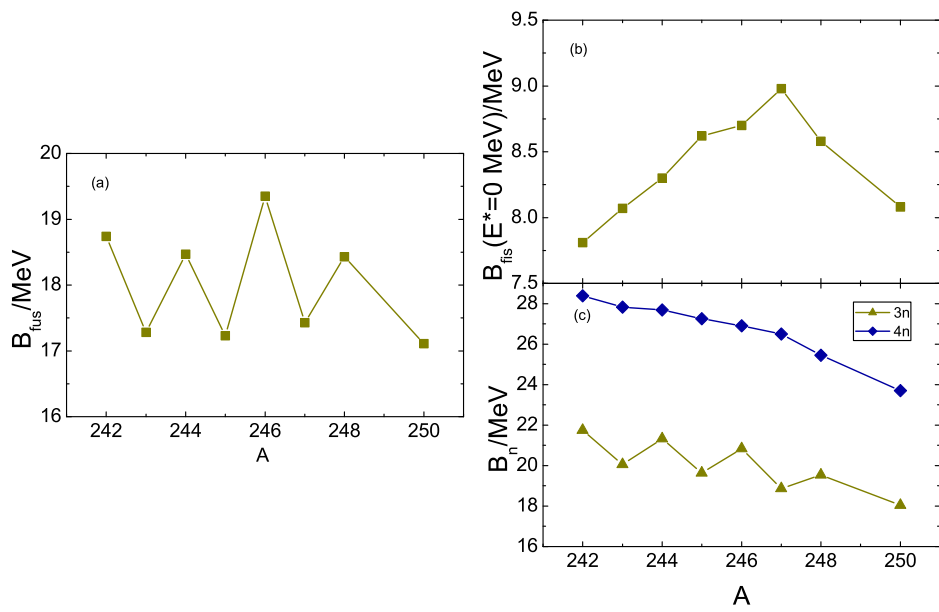


Figure 13: (a) the inner fusion barrier, (b) the fission barrier of the compound nucleus and (c) the neutron separation energy as a function of the mass numbers of the isotopic targets Cm in the reactions $^{48}\text{Ca} + ^A\text{Cm}$.

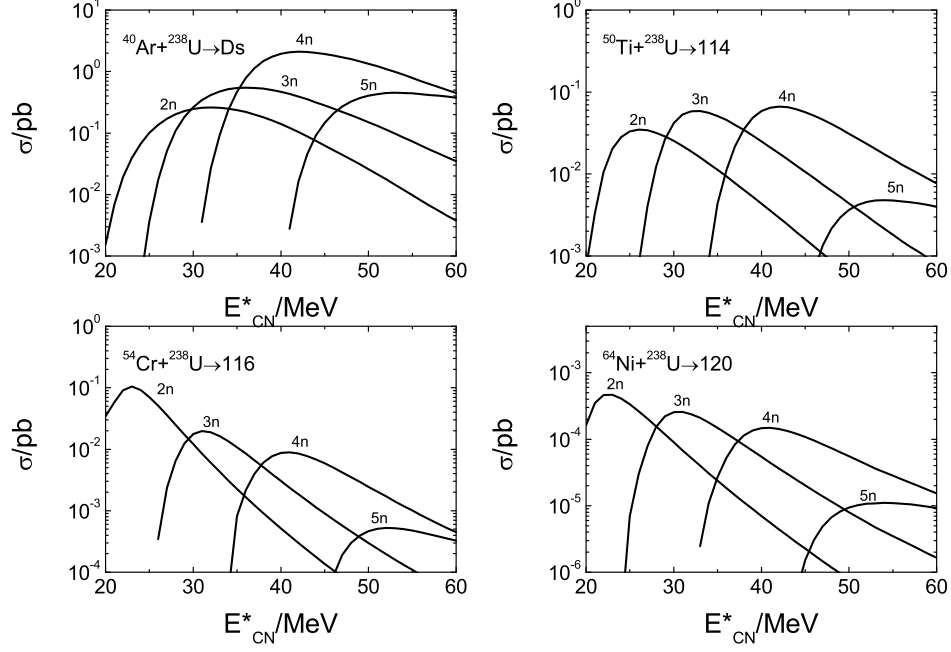


Figure 14: The evaporation residue excitation functions in the reactions ^{40}Ar , ^{50}Ti , ^{54}Cr , $^{64}\text{Ni}+^{238}\text{U}$.

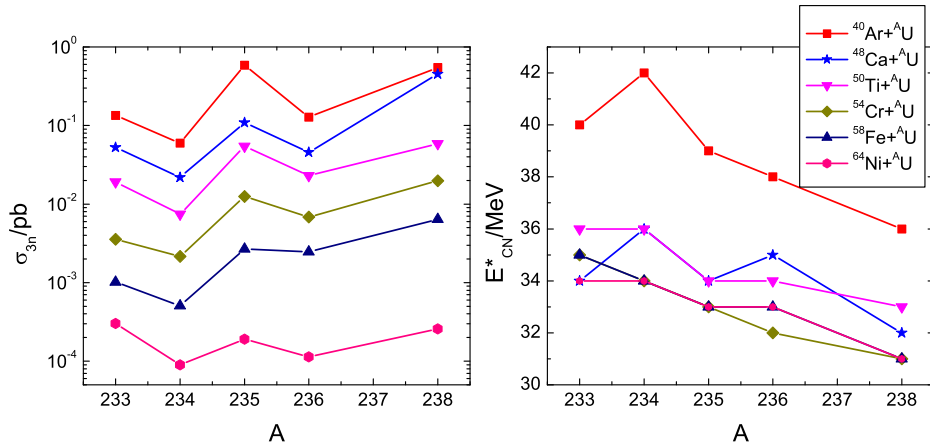


Figure 15: The production cross sections in the 3n channels as a function of the mass number of the isotopic targets U with projectiles ^{40}Ar , ^{48}Ca , ^{50}Ti , ^{54}Cr , ^{58}Fe and ^{64}Ni .